Molecular Cell, Vol. 12, 233–246, July, 2003, Copyright ©2003 by Cell Press

The Coordinated Functions of the *E. coli* MutS and MutL Proteins in Mismatch Repair

Samir Acharya,[1,*] Patricia L. Foster,[2] Peter Brooks,[3,4] and Richard Fishel[1,*]
[1] Genetics and Molecular Biology Program
Kimmel Cancer Center – BLSB 933
233 S. 10th Street, Philadelphia, Pennsylvania 19107
[2] Department of Biology
Jordon Hall 142
1001 E. Third Street
Indiana University
Bloomington, Indiana 47405
[3] Genoscope
Centre National de Sequencage
BP 191
2 rue Gaston Cremieux
91006 EVRY
France

Summary

The *Escherichia coli* MutS and MutL proteins have been conserved throughout evolution, although their combined functions in mismatch repair (MMR) are poorly understood. We have used biochemical and genetic studies to ascertain a physiologically relevant mechanism for MMR. The MutS protein functions as a regional lesion sensor. ADP-bound MutS specifically recognizes a mismatch. Repetitive rounds of mismatch-provoked ADP→ATP exchange results in the loading of multiple MutS hydrolysis-independent sliding clamps onto the adjoining duplex DNA. MutL can only associate with ATP-bound MutS sliding clamps. Interaction of the MutS-MutL sliding clamp complex with MutH triggers ATP binding by MutL that enhances the endonuclease activity of MutH. Additionally, MutL promotes ATP binding-independent turnover of idle MutS sliding clamps. These results support a model of MMR that relies on two dynamic and redundant ATP-regulated molecular switches.

Introduction

Mismatched nucleotides arise from polymerase misincorporation errors, recombination between heteroallelic parental DNAs, and chemical or physical DNA damage. The initiation of postreplication mismatch repair (MMR) in *E. coli* requires the MutS, MutL, MutH, and DNA adenine methylase (Dam) proteins (for review see Modrich and Lahue, 1996). Excision-resynthesis is accomplished by directing MMR to the newly replicated error-containing DNA strand via recognition of transiently undermethylated GATC Dam sites. Only MutS (MSH) and MutL (MLH) homologs appear to have been conserved throughout evolution (for review see Kolodner, 1996). Mutation of hMSH2 and hMLH1 account for the majority of hereditary nonpolyposis colorectal cancer (HNPCC) families (for review see Muller and Fishel, 2002, and references therein).

The mechanism of MMR is uncertain. Both MSH and MLH proteins contain consensus NTP binding domains and exhibit ATPase activity (Ban and Yang, 1998a; Haber and Walker, 1991). The MutS homologs belong to the Walker A/B sequence motif of NTPase families (Walker et al., 1982), while the MutL homologs belong to the unrelated GHKL or Bergerat-fold ATPase/kinase family (Bergerat et al., 1997; Mushegian et al., 1997). Debate about the MMR mechanism centers on the role of ATP hydrolysis and the mode of signal transduction between mismatched nucleotides and the excision machinery (Fishel et al., 2000).

Foundational studies by Modrich and colleagues revealed that MutS specifically bound mismatched DNA (Su and Modrich, 1986). In the presence of MutL and ATP, the MutS protein protection footprint on a mismatch was expanded (Grilley et al., 1989) and a MutH-dependent endonuclease activity at a hemi-methylated GATC site was activated (Welsh et al., 1987). The MutH incision was found to direct unwinding and degradation of the unmethylated DNA strand by the coordinated action of UvrD helicase and one of four ssDNA exonucleases (RecJ, ExoI, ExoVII, and ExoX [Matson, 1986; Viswanathan and Lovett, 1998; Yamaguchi et al., 1998]). Depending on the location of the MutH incision relative to the mismatch, the resulting excision gap occurred in either direction but invariably traversed only the interval between a Dam site to just past the mismatch (Cooper et al., 1993; Grilley et al., 1993). Resynthesis of the resulting single-stranded gap appeared to be performed by the Pol III holoenzyme (Lahue et al., 1989).

Based on these studies an MMR mechanism was proposed, which we term the Hydrolysis-Dependent Translocation Model (Modrich, 1989; Modrich and Lahue, 1996). It posits the assembly of an MutS-MutL complex at the mismatch which motors via ATP hydrolysis bidirectionally, creating a looped structure (Allen et al., 1997). Such a DNA tracking process was envisioned to link MutS mismatch recognition with MutH endonuclease activity at a nearby GATC site as well as to provide directionality for subsequent loading of UvrD helicase and a ssDNA exonuclease.

Studies of the human MSH proteins led to a second mechanism which we term the Molecular Switch Model (see Fishel et al., 2000). It is based on the relatively recent observation that hMSH heterodimeric complexes (hMSH2-hMSH6 or hMSH2-hMSH3) display significant mismatch-dependent ATPase activity (Gradia et al., 1997; Wilson et al., 1999). ATP binding by hMSH proteins was shown to result in the formation of a DNA sliding clamp capable of hydrolysis-independent diffusion for several thousand nucleotides (Gradia et al., 1999). Iterative loading of multiple sliding clamps was proposed to mark the mismatch region as well as to provide a directional gradient of clamps along the DNA duplex surrounding the mismatch site (Gradia et al., 1999; Heinen et al., 2002). ATP hydrolysis only occurred when

*Correspondence: rfishel@lac.jci.tju.edu (R.F.), s_acharya@lac.jci.tju.edu (S.A.)
[4] Presently on leave of absence from CNRS at IntegraGen, 4, rue Pierre Fontaine, 91000 Evry, France.

the hMSH proteins dissociated from the DNA ends (Gradia et al., 1999). These observations accounted for their low ATPase activity (Gradia et al., 1997, 2000; Haber and Walker, 1991; Hess et al., 2002) and identified the rate-limiting step as exchange of bound ADP for ATP at the mismatch site rather than ATP hydrolysis during translocation. This process appeared remarkably similar to the control of G protein molecular switches by GDP→GTP exchange (for review see Sprang, 1997). Based on these results a modification of the Hydrolysis-Dependent Translocation Model was introduced, which incorporated a two-site ATPase, although ATP hydrolysis was still required to propel movement along the DNA (Blackwell et al., 1998b).

The MutS structure revealed a homodimer clamped around a mismatched DNA substrate (Lamers et al., 2000; Obmolova et al., 2000) that largely confirmed previously predicted hinge and clasp domains (Guerrette et al., 1998). Only the nucleotide-free and ADP-bound forms of MutS have been solved, since infusion of ATP or ATPγS disintegrates the MutS crystal (Junop et al., 2001). These observations suggest conformational transition(s) occur upon ATP binding. Structural analysis of an N-terminal MutL fragment (Ban and Yang, 1998a), combined with peptide-mapping studies of the *S. cerevisiae* and human homologs (Guerrette et al., 1999; Tran and Liskay, 2000), suggested that MutL might form an ATP-dependent clamp-like structure similar to topoisomerase II (Berger and Wang, 1996).

Computer-predicted protein-protein interfaces of MutS, MutL, and MutH (Ban and Yang, 1998a, 1998b; Lamers et al., 2000; Obmolova et al., 2000) led to a third MMR mechanism that we term the Static Transactivation Model (Junop et al., 2001). In this model, a DNA scanning process concludes with a mismatch interaction that enhances the lifetime of ATP-bound MutS, which leads to the formation of a static MutS-MutL-MutH complex on or near the mismatch DNA site. This heterotrimeric complex (bound to DNA) was suggested to collide in *trans* with a GATC site, provoking MutH endonuclease incision (Junop et al., 2001; Schofield et al., 2001). It was not immediately evident how such a random collision in three-dimensional space could direct an excision tract from the Dam site toward the mismatch site. The commonly observed ATP-dependent release of MutS from a mismatch in the absence of MutL and/or MutH was considered an abortive repair event.

Here we have addressed the inconsistencies between the MMR models by developing physiologically relevant biochemical reactions. We detail the mechanism of MutS and MutL in the activation of MutH and confirm these results with genetic studies. Our results refine the Molecular Switch Model and define the role of ATP in the complex processes of MMR.

Results

The MutS Protein Contains an Intrinsic Mismatch-Dependent ATPase Activity

Most previous studies of MSH ATPase activity have been performed under nonphysiological conditions that include salt concentrations at or below 50 mM (Alani et al., 1997; Biswas et al., 2001; Blackwell et al., 2001a), at 200 mM (Drotschmann et al., 2002), or in the absence of DNA (Junop et al., 2001). Using a model 41-mer, we found that the MutS protein displayed a mismatched DNA-stimulated ATPase activity that was dependent on salt concentration (Figure 1A). Maximal stimulation of the mismatch-dependent MutS ATPase activity occurred between 100 and 160 mM NaCl (Figure 1A); notably, this is the consensus physiological salt range (Record et al., 1998; Schultz and Solomon, 1961) and the optimum for the complete MMR reaction in vitro (Blackwell et al., 1998a). Below 50 mM and above 250 mM salt, there is no discrimination between mismatched and duplex DNA (Figure 1A). Both the yeast and human MSH ATPases display a similar salt dependence (Gradia et al., 2000; Hess et al., 2002).

We examined the stimulation of the MutS steady-state ATPase by Michaelis-Menten analysis in the presence of a G/T mismatch ($k_{cat}/K_m = 0.23\ \mu M^{-1}\cdot min^{-1}$; $K_m = 23 \pm 2.2\ \mu M$), a G/C control duplex ($k_{cat}/K_m = 0.1\ \mu M^{-1}\cdot min^{-1}$; $K_m = 31 \pm 5.1\ \mu M$), or in the absence of DNA ($k_{cat}/K_m = 0.09\ \mu M^{-1}\cdot min^{-1}$; $K_m = 20 \pm 1.2\ \mu M$) (Figure 1B). These results are qualitatively similar to the yeast and human MSH proteins (Gradia et al., 1997; Hess et al., 2002; Wilson et al., 1999).

The steady-state ATPase cycle can be conceptually divided into γ-phosphate hydrolysis and the release of ADP prior to ATP binding. As with the hMSH proteins, we found no difference in the rate of single-step γ-phosphate hydrolysis in the presence of a G/T mismatch, G/C duplex, or in the absence of DNA (see Gradia et al., 1997 for method; data not shown). These results suggest that the MutS ATPase is unlikely to be controlled by γ-phosphate hydrolysis at physiologically relevant salt concentrations.

We examined ADP release by prebinding MutS with [^{3}H]-ADP and measuring the kinetic loss of ADP following the addition of excess unlabeled ATP plus DNA (where indicated). We observed significantly accelerated ADP release in the presence of the G/T mismatch ($t_{1/2} < 5$ s) compared to the G/C duplex ($t_{1/2} \approx 10$ s) or to the absence of DNA ($t_{1/2} \approx 30$ s) (Figure 1C). Little or no ADP was released in the absence of exogenous ATP (data not shown). These results suggest that ADP release is facilitated by a mismatch and concurrent ATP binding (ADP→ATP exchange).

The amount of ADP→ATP exchange by MutS in the absence of DNA and in the presence of G/C duplex was surprising (Figure 1C). These results contrast with the hMSH proteins, which show very little ADP→ATP exchange in the absence of DNA and at least a 20-fold reduction in the rate of ADP→ATP exchange in the presence of G/C duplex DNA compared to G/T mismatched DNA (Gradia et al., 1997; Wilson et al., 1999; unpublished data). To determine whether DNA ends might contribute to these differences, we examined ADP→ATP exchange using oligonucleotide DNA substrates in which both ends were blocked with biotin-streptavidin. The rate of ADP→ATP exchange in the presence of double blocked-end G/T mismatch DNA appeared largely unaffected ($t_{1/2} < 5$ s; Figure 1D), but the rate of exchange in the presence of double blocked-end G/C duplex DNA now appeared identical to the rate in the absence of DNA ($t_{1/2} \approx 30$ s). These observations suggest that MutS ADP→ATP exchange and consequent ATPase activity are activated by exposed DNA ends, a condition that is

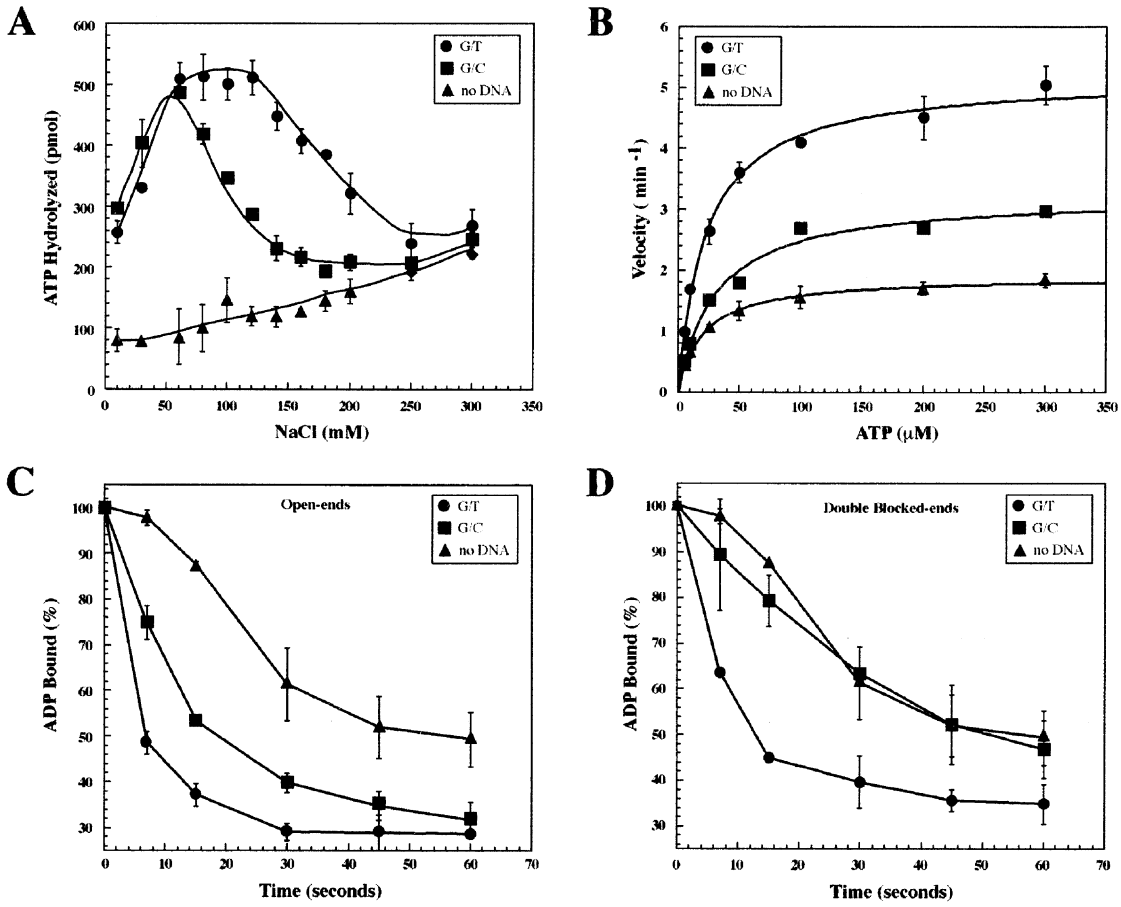

Figure 1. Mismatch-Dependent Activation of the MutS ATPase and ADP→ATP Exchange Activities

The ATPase and ADP→ATP exchange assays were performed without DNA (▲), with G/C control DNA (●), or with G/T mismatch DNA (■).

(A) Effect of salt on the MutS ATPase activity. Reactions were performed with 100 nM MutS and 300 nM DNA.

(B) Kinetic analysis of the MutS ATPase. Assays were performed as in (A) with MutS (50 nM; in the presence of DNA) and MutS (100 nM; in the absence of DNA) at 140 mM NaCl. The velocity of the reaction is plotted as a function of ATP concentration, and the curves were fitted to the Michaelis-Menten equation (Gradia et al., 2000).

(C) ADP→ATP exchange by MutS. Reactions were performed with MutS (100 nM) and open-ended oligonucleotide DNA substrate (100 nM; where indicated). The MutS protein was preincubated with 3 μM [^{3}H]-ADP on ice. The release of bound [^{3}H]-ADP was monitored following the addition of 25 μM ATP and DNA (where indicated).

(D) Same as (C) except biotin-streptavidin double blocked-end DNA was substituted for the open-ended DNA. Standard deviations were calculated from at least three independent experiments.

likely to be rare in vivo. Together these results suggest that mismatch-provoked ADP→ATP exchange is a determining factor in MutS recognition specificity.

MutS Functions as a Mismatch-Dependent Molecular Switch

Mismatched DNA binding studies with MutS have been largely performed at or below 50 mM salt (Allen et al., 1997; Biswas et al., 2001; Blackwell et al., 2001a; Jiricny et al., 1988; Su and Modrich, 1986). We examined MutS mismatch binding at physiological salt using the IAsys Total Internal Reflectance (TIR) system. The TIR system measures changes in the refractive index induced by the accumulation of mass on a measuring surface and correlates with real-time binding isotherms in a closed-cuvette system under conditions of continuous equilibrium. TIR differs significantly from the continuous-flow Biacore plasmon resonance system in which equilibrium binding must be theoretically extrapolated. We used a model 82-mer (containing the core 41-mer sequence) for these and all subsequent DNA binding studies to control for an apparent DNA length-dependence associated with MutS-MutL complex formation (Blackwell et al., 2001b; data not shown).

We observed significant binding of MutS to a G/T mismatch ($t_{1/2} \approx 60$ s; $K_D = 16$ nM) compared to G/C duplex DNA (Figure 2A). Nonspecific association with the DNA end accounts for the majority of binding to the G/C duplex DNA (Supplemental Data, http://www.molecule.org/cgi/content/full/12/1/233/DC1; Supplemental Figure S1). The MutS•G/T mismatch complex was stable to buffer replacement that removes unbound MutS (Figure 2A) as well as to the addition of 500 μM ADP (data not shown). Our observations appeared qualitatively similar to Blackwell et al. (2001a), except that we were unable to detect any mismatched or duplex DNA binding in presence of ATP or ATPγS. It is likely that many of these differences may be traced to the

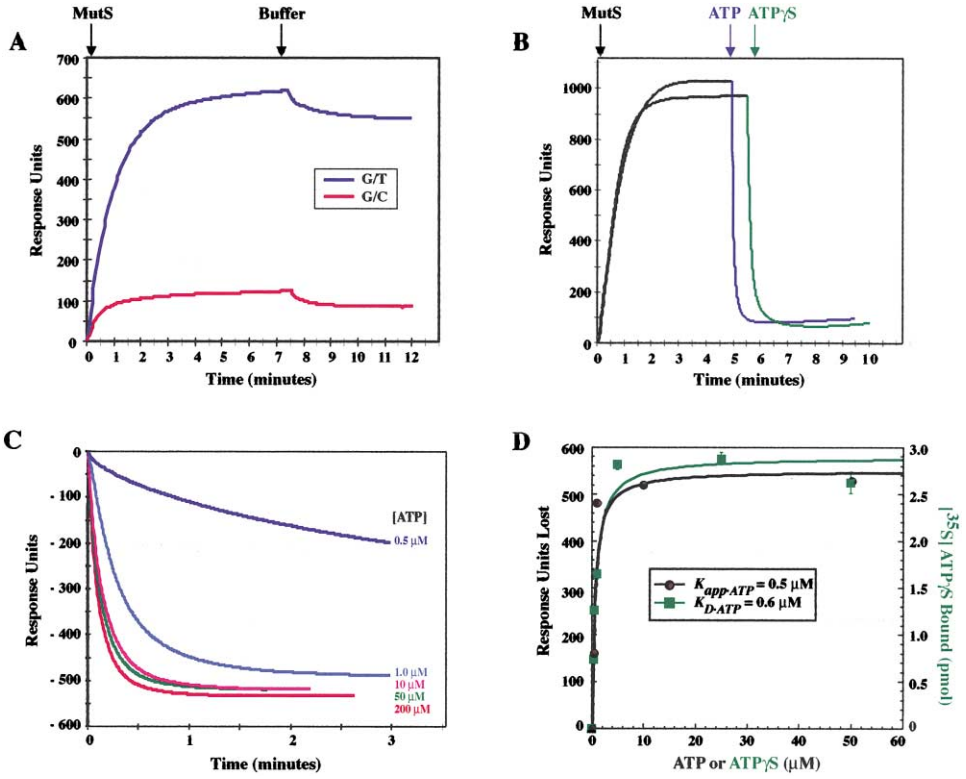

Figure 2. Interdependent Modulation of MutS Mispair Binding and ATP Binding

Total Internal Reflectance (TIR) real-time binding and dissociation isotherms of MutS to an 82-mer DNA were measured using the IASys system. Binding of MutS to DNA is reflected in the increase in response units with time. (A) Binding specificity of MutS. Binding was initiated by the addition of MutS (200 nM) to a cuvette containing the G/T mismatch DNA (blue tracing) or G/C control DNA (red tracing). Following binding, the solution was replaced with an identical buffer except without MutS or nucleotide. The stability of the bound fraction was monitored over time. Multiple TIR binding experiments using variable concentrations of MutS protein were performed to determine association ($k_{assoc.}$) and dissociation ($k_{dissoc.}$) constants. From these values, an equilibrium dissociation constant (K_D) was calculated for the interaction of MutS with a G/T mismatch.

(B) The effect of ATP and ATPγS on the stability of the MutS bound to G/T mismatch DNA. TIR binding of MutS to G/T mismatch DNA was performed as in (A). Following binding the buffer was replaced with an identical buffer that included 1 mM ATP (blue trace) or ATPγS (green trace) and the effect monitored over time.

(C) TIR dissociation isotherms of MutS as a function of ATP concentration. MutS protein was bound to a G/T mismatch DNA as in (A). Unbound MutS was removed and dissociation of MutS initiated by the addition of the indicated amount of ATP. The resulting loss in the response units of bound MutS was monitored over time.

(D) Comparison of dissociation constants for ATP-dependent release from a G/T mismatch and ATP binding in the presence of G/T mismatched DNA. Response units lost at 2 min (●, black) and the binding of MutS (300 nM) to [^{35}S]-ATPγS in the presence of G/T mismatched DNA (■, green) were plotted as a function of ATP concentration. The resulting curves were fitted to a hyperbolic plot and the $K_{app,ATP}$ for ATP-dependent release and $K_{d,ATP}$ for DNA-independent ATPγS binding determined (shown in box). Standard deviation was calculated from at least three independent experiments.

continuous-flow Biacore system, the substantially altered binding kinetics, and/or nonphysiological salt conditions. The MutL protein does not appear to bind ssDNA, dsDNA, or mismatched DNA at physiologically relevant salt concentrations (data not shown). These results contrast with those of the yeast MLH proteins performed at 25 mM salt (Hall et al., 2001).

When ATP or ATPγS is added to MutS prebound to the G/T mismatch, the MutS protein rapidly dissociates from the DNA ($t_{1/2} < 5$ s; Figure 2B). These results demonstrate ATP/ATPγS-dependent, but hydrolysis-independent, dissociation of MutS from mismatched DNA. We determined the concentration of ATP and ATPγS that resulted in half-dissociation of MutS from G/T mismatch DNA (Figure 2C and data not shown; $K_{app•ATP} = 0.5$ μM, plotted in black in Figure 2D; identical for ATPγS, data not shown) and compared it to the ATPγS binding affinity of MutS in the presence of the G/T mismatched DNA ($K_{D•ATP} = 0.6$ μM, plotted in green in Figure 2D). The correlation between $K_{app•ATP}$ and $K_{D•ATP}$ together with the ADP→ATP exchange and ATPase data (Figure 1) are consistent with the conclusion that interaction of MutS with mismatched DNA provokes releases of bound ADP, consequent binding of ATP, dissociation from a mismatch, and the initiation of the MutS ATPase cycle.

MutL Only Forms a Specific Complex with ATP-bound MutS Clamps

Previous studies that projected an interaction between bacterial, yeast, and human MSH and MLH proteins have exhibited a variety of conflicting conditions, interaction partners, and DNA dependence (Galio et al., 1999; Gu et al., 1998; Habraken et al., 1998; Plotz et al., 2002; Prolla et al., 1994; Raschle et al., 2002; Schofield et al., 2001; Spampinato and Modrich, 2000). We hypothesized that the incongruities might be traced to three variable

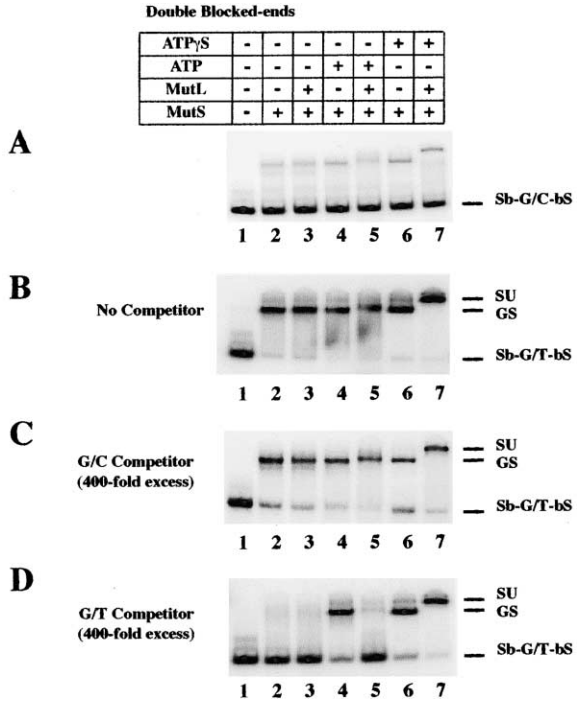

Figure 3. Examination of an MutS-MutL Gel Shift Complex on Blocked-End G/T Mismatch DNA

MutS-MutL interaction on 82 bp biotin-streptavidin double blocked-end G/T mismatch DNA. Binding was initiated by the addition of MutS (100 nM) followed by sequential addition of ATP or ATPγS (1 mM) and MutL (100 nM). Where indicated, a 400-fold excess of unlabeled 82 bp G/T mismatch DNA or G/C duple competitor was added after MutL incubation. Gel shift analysis was performed on a 5% native PAGE (see Experimental Methods).

(A) MutS/MutL binding to biotin-streptavidin double blocked-end G/C control DNA (Sb-G/C-bS).

(B) MutS/MutL binding to biotin-streptavidin double blocked-end G/T mismatch DNA (Sb-G/T-bS).

(C) Same as (B) except that a 400-fold excess unlabeled 82 bp G/C control DNA competitor was added following binding incubation (and further incubated 10 min).

(D) Same as (B) except that a 400-fold excess unlabeled 82 bp G/T mismatch DNA competitor was added following binding incubation (and further incubated 10 min). The migration positions of the biotin-streptavidin double blocked-end G/C control DNA (Sb-G/C-bS); the biotin-streptavidin double blocked-end G/T mismatch DNA (Sb-G/T-bS); the MutS-G/T mismatch DNA complex (GS); the MutS-MutL-G/T mismatch super-shifted complex (SU) are indicated.

factors: nonphysiological salt conditions, inadequately characterized adenosine nucleotide bound/free forms of MutS, or open-ended DNA substrates.

We performed DNA binding and complex formation studies between MutS and MutL using a biotin-streptavidin double blocked-end DNA substrate at physiological salt concentration (Figures 3A–3D). In the absence of adenosine nucleotide (data not shown) or in the presence of ADP, MutS formed a quantitative and specific gel shift (GS) complex on double blocked-end G/T mismatch DNA (Figure 3B, lane 2) compared to a double blocked-end G/C duplex DNA (<5%; Figure 3A, lane 2). The MutS GS complex on the double blocked-end G/T mismatch DNA was stable to the subsequent addition of a 400-fold excess of unlabeled G/C duplex competitor (Figure 3C, lane 2) but was completely eliminated after the addition of a 400-fold excess of unlabeled G/T competitor (Figure 3D, lane 2). These results are consistent with previous studies (Jiricny et al., 1988) and demonstrate both specificity and reversibility of mismatch-recognition by MutS. The addition of MutL to this basic MutS binding reaction did not alter the specificity or reversibility exhibited by the MutS GS complex (Figures 3B–3D, lane 3). We conclude that MutL does not significantly interact with or affect MutS that is bound to a mismatch.

The MutS GS complex was retained on double blocked-end G/T mismatch DNA in the presence of ATP or ATPγS (Figure 3B, lanes 4 and 6). This complex was largely unaffected by the subsequent addition of either excess unlabeled G/C competitor or G/T competitor (Figures 3C and 3D, lanes 4 and 6). The complete resistance of the MutS GS complex to competitor DNA is most consistent with the formation of an irreversible ATP-bound MutS clamp that is trapped on the double blocked-end G/T mismatch DNA (Blackwell et al., 2001a; Gradia et al., 1999). We also found that the steady-state MutS ATPase in the presence of double blocked-end mismatched DNA was reduced to a background similar to that without DNA (data not shown). Since ADP→ATP exchange readily occurs on double blocked-end mismatched DNA (Figure 1D), we conclude that dissociation from open ends is required to complete the ATPase cycle (γ-phosphate hydrolysis).

The step-wise addition of MutL to MutS clamps formed in the presence of ATP did not appear to alter significantly the mobility of the GS complex on blocked-end G/T mismatch DNA (Figure 3B, compare lanes 4 and 5). Furthermore, subsequent addition of excess unlabeled G/C competitor did not affect the stability of this GS complex (Figure 3C, lane 5). However, the addition of excess unlabeled G/T competitor resulted in the complete elimination of the GS complex (Figure 3D, lane 5). This pattern appeared similar to the reversibility of MutS mismatch binding in the absence of ATP (see Figure 3D, lane 2), suggesting that MutL induces reversibility of the MutS GS complex formed in the presence of ATP without affecting the specificity for mismatched DNA.

In contrast, the step-wise addition of MutL to MutS clamps formed in the presence of ATPγS resulted in a quantitatively supershifted (SU) complex (Figures 3B–3D, lane 7) that remained stably bound in the presence of excess unlabeled G/T competitor (Figure 3D, lane 7). These results suggest that the MutL-induced reversibility of the ATP-bound MutS GS complex requires ATP hydrolysis. The formation of a SU complex is consistent with the conclusion that MutS-MutL is trapped in an irreversible ternary complex in the absence of ATP hydrolysis. Interestingly, a ternary complex between G proteins and their corresponding GAPs is stabilized by GTPγS (Sprang, 1997). These observations are most consistent with the hypothesis that MutL only interacts with ATP- or ATPγS-bound MutS clamps and may then induce ATP hydrolysis-dependent turnover.

ATP Binding and Hydrolysis by MutL are not Required for Either the Interaction with or Turnover of MutS Sliding Clamps

Since the gel shift studies could not address the individual roles of ATP binding/hydrolysis by MutS or MutL, we developed a double blocked-end DNA substrate for

TIR by annealing a 5′ biotin oligonucleotide with an oligonucleotide containing 5′ fluorescein. The biotinylated end was attached to the TIR surface via streptavidin, and anti-fluorescein antibodies were used to block the remaining duplex end. We found that the MutS protein bound the biotin/fluorescein (b/f) double blocked-end G/T mismatch substrate as efficiently as a single-end biotinylated G/T mismatch attached to the TIR surface (compare Figures 4A and 2A).

The individual ATP binding activities were examined by changing solution conditions in step-wise manner. As with an open-ended DNA substrate, replacement of the initial binding buffer with MutS-free buffer did not significantly reduce the amount of MutS bound to the G/T mismatch (compare Figures 2A and 4A). Furthermore, there was no increase in mass on the TIR surface following step-wise addition of MutL to the MutS-bound b/f double blocked-end G/T mismatch DNA (Figure 4A). These results confirm the gel shift studies (Figures 3B–3D, lane 3) and are consistent with the conclusion that MutL does not interact with and/or affect a MutS homodimer that is bound at the G/T mismatch (Figure 4A)

We examined the effect of ATP or ATPγS on MutL association with MutS clamps (Figure 4B). Following the initial binding (see "MutS," Figure 4B, tracings 1–5), the reaction solution was replaced with a buffer containing ATP or ATPγS (see "MutS Dissn. ATP/ATPγS," Figure 4B, tracings 1–5). For all the reactions shown in Figure 4B, no more than 10%–20% of the initially bound MutS was released. These results demonstrate that the majority of b/f G/T mismatch DNA contained double blocked-ends that trapped ATP- or ATPγS-bound MutS clamps. An apparently nonspecific mass increase in the presence of ATP (but not ATPγS) (Figure 4B, tracings 1–3) was eliminated by a nucleotide-free buffer wash (see "Buffer wash," Figure 4B, tracings 1–3). Together, these results suggest that TIR may be used to visualize the formation and processing of ATP- or ATPγS-bound MutS clamps

Unlike MutS bound to a mismatch (Figure 4A), the addition of MutL protein to trapped ATP- or ATPγS-bound MutS sliding clamps produced a significant mass increase (see "MutL Assn.," Figure 4B, tracings 1-5; compared to Figure 4A, "MutL"). By comparison with Figure 4A, these results imply that MutL only interacts with ATP- or ATPγS-bound MutS clamps. The on-rate (k_{on}) of MutL with ATP- or ATPγS-bound MutS clamps ($k_{on} \approx 2.8\ min^{-1}$) appears equivalent to the association of MutS with mismatched DNA ($k_{on} \approx 2.6\ min^{-1}$) and does not require exogenous ATP (Figure 4B, tracing 1; data not shown). However, the MutS-MutL complex appears to be maintained by the inclusion of exogenous ATP with the MutL (compare the gradual loss of mass in Figure 4B, tracing 1, with the stability of Figure 4B, tracing 2). These observations are consistent with previous results (Galio et al., 1999; Figure 3) and suggest that MutL promotes the turnover of MutS clamps that may rapidly reform in the presence of exogenous ATP.

To test this hypothesis, we introduced excess G/T mismatch competitor (see "G/T Competitor," Figure 4B, tracings 1–5). We observed a kinetic loss of mass only when the MutS clamps were initially formed with ATP (Figure 4B, tracings 1–3). The MutS clamps formed with ATPγS were stable to exogenous G/T competitor regardless of whether ATP or ATPγS was included with MutL (Figure 4B, tracings 4 and 5). These results suggest that clamp release occurs by intrinsic MutS ATP hydrolysis that is accelerated by MutL and refractory for ATPγS-bound MutS clamps. In support of this hypothesis, we observed insensitivity to exogenous G/T competitor by

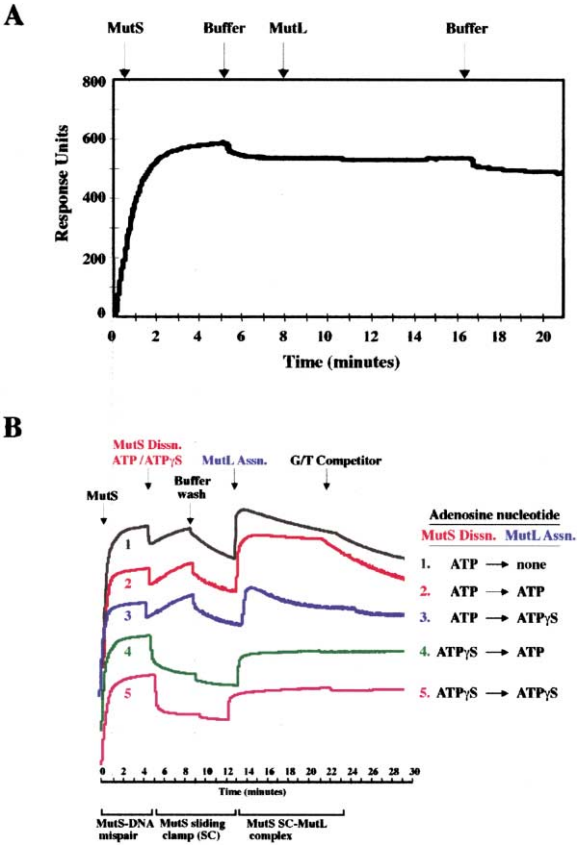

Figure 4. ATP Binding/Hydrolysis by MutL Are Not Required for Interaction with ATP-Bound MutS Sliding Clamps

(A and B) Real-time TIR analysis of the MutL interaction with MutS bound to G/T mismatch DNA was performed using IASys. (A) The MutS protein (200 nM) was bound to G/T mismatch DNA in buffer B (marked "MutS"). The unbound material was removed by replacement with buffer B without MutS protein (marked "Buffer"). At approximately 9 min, MutL (200nM final) in buffer B was added (marked "MutL"). At approximately 17 min, the unbound material was removed by replacement with buffer B without protein (marked "Buffer"). Note the stability of the MutS-G/T mismatch complex over the course of 20 min (loss of no more than 3%–5% of initial response units). (B) The addition of MutL to trapped MutS sliding clamps. The individual effect of ATP or ATPγS on MutS-MutL complex formation was determined. The MutS (200 nM) was bound to the b/f double blocked-end G/T mismatch DNA (marked "MutS") as in (A). The binding for each of the five curves was similar to (A) and the axis was eliminated here to facilitate comparison. Replacement of the binding buffer with buffer B containing ATP or ATPγS traps MutS sliding clamps bound to b/f double blocked-end G/T mismatch DNA (marked "MutS Dissn. ATP/ATPγS"). The unbound material was removed by replacement with buffer B without MutS protein or adenosine nucleotide (marked "Buffer wash"). The MutL protein (200nM final) in buffer B was then added (marked "MutL Assn") with or without ATP or ATPγS (1 mM). After 10 min, an approximately 50-fold excess of 82 bp G/T mismatch DNA was added (marked "G/T Competitor"). Predicted protein configuration(s) are indicated in brackets below tracings. Adenosine nucleotide content for each tracing at the "MutS Dissn." and "MutL Assn." steps is indicated in right insert.

MutS sliding clamps formed in the presence of ATP when subsequent MutL addition included ATPγS (Figure 4B, tracing 3). We conclude that ATP-bound MutS clamps released by MutL may reform as ATPγS-bound MutS clamps in the TIR closed system (see initial release and then stabilization of mass in Figure 4B, tracing 3). Once the majority of ATP-bound MutS clamps are recycled to ATPγS-bound MutS clamps, they become insensitive to exogenous G/T competitor (Figure 4B, tracing 3). Taken as a whole these results suggest that ATP binding and hydrolysis by MutL are not required for MutS sliding clamp interaction or turnover.

The estimated off rates (k_{off}) for the various protein-DNA and protein-protein complexes were as follows: MutS·ATP sliding clamp on blocked-end DNA ($k_{off} \approx 0.03\ min^{-1}$) << MutS-G/T mismatch ($k_{off} = 0.2\ min^{-1}$) ≈ MutS·ATP-MutL ($k_{off} \approx 0.5\ min^{-1}$) << MutS•ATP sliding clamp on open-ended DNA ($k_{off} \approx 9\ min^{-1}$). These observations place the rate of MutL-dependent removal of ATP-bound MutS sliding clamps in the same order of magnitude as the dissociation of MutS from a mismatch, but at least 10-fold faster than the intrinsic dissociation of trapped ATP-bound MutS sliding clamps from blocked-end DNA.

MutL Functions as a MutH-activated Molecular Switch

We determined that multiple ATP-bound MutS sliding clamps were iteratively loaded onto a circular DNA containing a G/T mismatch which may then form multiple MutS-MutL complexes (Supplemental Data; Supplemental Figure S2A). Moreover, both MutS and MutS-MutL complexes appeared capable of ATP hydrolysis-independent diffusion of at least 1 kb along duplex DNA (Supplemental Data; Supplemental Figures S2B and S2C; see Figure 5D). To facilitate biochemical as well as genetic studies, we reconstructed three previously described site-specific mutations of MutL in conserved ATPase domains of the Bergarat-fold [MutL(E29A); MutL(R95F); MutL(N302A); Ban et al., 1999]. These mutations did not complement the mutator phenotype exhibited by an *E. coli mutL* strain nor did the purified mutant proteins display measurable ATPase activity (data not shown; Ban et al., 1999). Furthermore, we observed no significant ATP binding by the MutL(E29A) or MutL(R95F) proteins (Figure 5A; Ban et al., 1999). However, to our surprise the MutL(N302A) protein displayed enhanced ATP binding activity ($K_D = 20\ \mu M$) compared to wild-type MutL ($K_D = 90\ \mu M$; Figure 5A). These observations contrast with those of Ban et al. (1999) and are likely to be the result of a second mutation (R95F) found in the original construct (unpublished data; Junop et al., 2001).

We found no difference between the MutL(E29A), MutL(R95F), and MutL(N302A) proteins compared to the wild-type MutL with respect to (1) release/turnover of MutS sliding clamps (Figure 5B, compare lane 6 with related controls in lanes 1–5), (2) formation of an SU complex with MutS in the presence of ATPγS on double blocked-end G/T mismatch DNA (Figure 5C, compare lanes 4–7 with related controls in lanes 1–3), or (3) hydrolysis-independent diffusion of the ATPγS-bound MutS-MutL complex off a G/T mismatch substrate (Figure 5D, compare lanes 6–13 with lanes 1–5; see also Supplemental Data and Supplemental Figure S2). These results parallel the TIR studies (Figure 4B) and support the conclusion that ATP binding and hydrolysis are not required for MutL to interact with MutS and/or promote turnover of MutS sliding clamps.

Purified MutH protein does not bind or hydrolyze ATP (data not shown). Furthermore, MutH does not affect MutS mispair binding activity, MutS or MutL ATPase activity, or the formation/release of the MutS-MutL complex (data not shown). However, MutH appeared to promote a significant dose-dependent increase in ATP binding by MutL ($K_D = 16\ \mu M$) that saturated at an equimolar ratio of the proteins (Figure 6A; data not shown).

The ATP binding activity of MutL in the presence of MutH appeared similar that of MutL(N302A) protein (compare Figures 5A and 6A). Moreover, the addition of MutH to MutL(N302A) did not further alter its ATP binding activity (data not shown). These results suggested that ATP binding by the MutL(N302A) protein might be constitutively activated. To test this possibility we examined MutH endonuclease activity on a hemimethylated oligonucleotide containing a single GATC site (Figure 6B). We determined that in the presence of ATP or ATPγS, MutL was capable of activating the MutH endonuclease (Figure 6B), although less efficiently than in the presence of MutS with a mismatch (data not shown). This minimal system allowed us to examine the ATP dependence of MutH activation by MutL without the complication associated with MutS ATP binding and/or ATPase activities.

Wild-type MutL activated the MutH endonuclease ($K_{app•ATP} = 130\ \mu M$; $V_{max} = 2.3$ fmol/hr), while MutL(R95F) protein did not (Figure 6B). As expected, the MutL(N302A) protein appeared substantially more efficient than wild-type for activation of the MutH endonuclease ($K_{app•ATP} = 52\ \mu M$; $V_{max} = 6$ fmol/hr) (Figure 6B). These results support the hypothesis that MutH provokes ATP binding by MutL, which in turn enhances MutH endonuclease activity.

Overexpression of MutL Results in a Dominant Mutator Phenotype

The MutS, MutL, and MutH proteins exist in approximately equimolar concentration in the bacterial cell (Feng et al., 1996). We examined the genetic effect(s) of altering cellular levels of the wild-type and mutant MutL proteins using an arabinose-inducible promoter (Guzman et al., 1995). Growth in arabinose resulted in overproduction of the wild-type and mutant MutL proteins in an *E. coli mutL* strain (Figure 6C) as well as in wild-type *E. coli*, although the background of endogenous wild-type MutL obscured accurate quantitation in the latter strain (data not shown). These results suggest that arabinose induction substantially increases the levels of the wild-type and mutant MutL proteins without significant protein degradation.

Following arabinose induction of MutL for 3–4 generations in wild-type *E. coli*, the frequency of Lac^+ mutants (reversion of a −1 bp frameshift; Cupples et al., 1990) was found to increase 56-fold over the vector alone (Figure 6D). These results suggest that overexpression of MutL is a dominant mutator. A similar overexpression

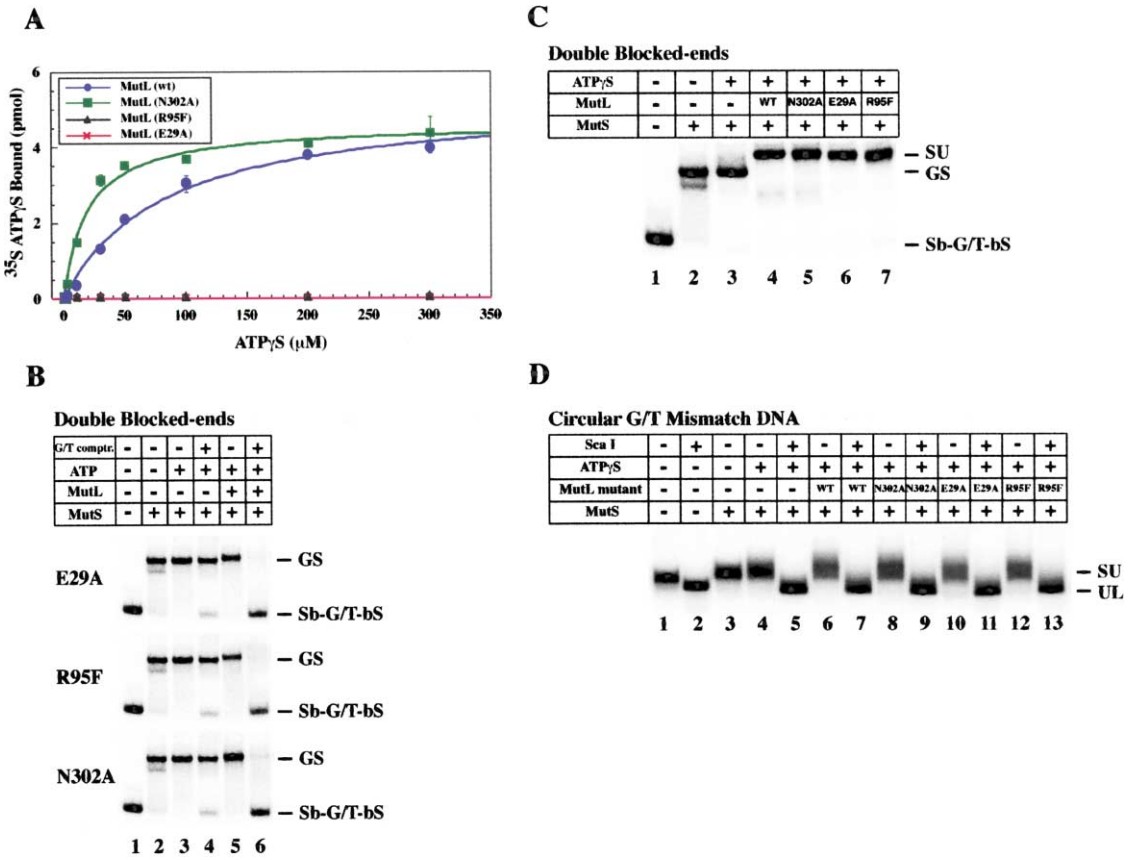

Figure 5. MutL ATP Binding/Hydrolysis Mutants Do Not Affect MutS Sliding Clamps Interaction/Release or Hydrolysis-Independent Diffusion of the MutS-MutL Sliding Clamp Complex

(A) The equilibrium binding of ATPγS by MutL mutant proteins. Filter binding was used to calculate the equilibrium disassociation constants (K_D) for [^{35}S]-ATPγS binding by wild-type MutL (●), MutL(N302A) (■), MutL(R95F) (▲), and MutL(E29A) (×).The curves were fitted to a hyperbolic plot and the disassociation constants calculated [MutL K_D = 90 μM; MutL(N302A) K_D = 20 μM; ATPγS binding to MutL(E29A) and MutL(R95F) was negligible].

(B) The effect of MutL ATP binding/hydrolysis mutant proteins on the release of MutS sliding clamps. Binding to the 82 bp biotin-streptavidin double blocked-end G/T mismatch DNA (Sb-G/T-bS) was initiated by the addition of MutS (100 nM) followed by sequential addition of ATP (1 mM), and MutL (100 nM) where indicated. A 400-fold excess of unlabeled 82 bp G/T mismatch DNA competitor was added after MutL incubation in reactions indicated. Gel shift analysis was performed on a 5% native PAGE. The MutL mutant type added to MutS is shown on the left. Release of the ATP-bound MutS sliding clamp shifted complex (GS) only in the presence of the MutL mutant proteins and excess G/T mismatch competitor ("G/T comptr.") indicates competent release activity.

(C) A stable MutS-MutL complex is formed by MutL ATP binding/hydrolysis mutant proteins. Gel shift analysis was performed as described in (B) except ATPγS was used exclusively instead of ATP.

(D) Hydrolysis-independent diffusion of MutS-MutL complexes formed with ATP binding hydrolysis MutL mutant proteins. Binding and MutS-MutL complex formation was performed as in (C) in the presence of ATPγS except that the 2.9 kb circular DNA containing a G/T mismatch (circular G/T DNA) was substituted for the 82 bp DNA and a 400-fold excess of control G/C competitor was present. Gel shift analysis was performed as in Figure S2. Following MutS-MutL complex formation [SU], the circular G/T DNA was linearized with ScaI and MutS-MutL complexes allowed to dissociate to an unshifted linear (UL).

of MutL(R95F) increased the frequency of Lac$^+$ reversion mutants throughout the experiment (including during uninduced growth) to a final level that was 540-fold above vector alone and 10-fold above wild-type MutL (Figure 6D). Since overexpression levels appeared identical, the escalation of Lac$^+$ reversion mutants produced by MutL(R95F) compared to wild-type MutL suggests an additional level of dominant mutator activity.

Overexpression of MutL(N302A) resulted in a slightly lower Lac$^+$ reversion frequency compared to overexpression of wild-type MutL (Figure 6D). However, during arabinose induction the number of bacterial colonies that retained the MutL(N302A) plasmid declined, suggesting that induction of the mutant protein was detrimental. Quantitative analysis revealed that the survival of bacterial cells containing the vector alone, wild-type MutL, and MutL(R95F) was insensitive to a wide range of arabinose-inducing conditions (Figure 6E). However, 80% of the cells containing MutL(N302A) did not survive even at very low arabinose concentrations (0.02%; Figure 6E). Moreover, the remaining 20% of survivors appeared to inactivate the arabinose-dependent overexpression of MutL(N302A) (data not shown). These observations suggest that overexpression of constitutively activated MutL(N302A) was lethal. We conclude that relative protein levels are important for proper muta-

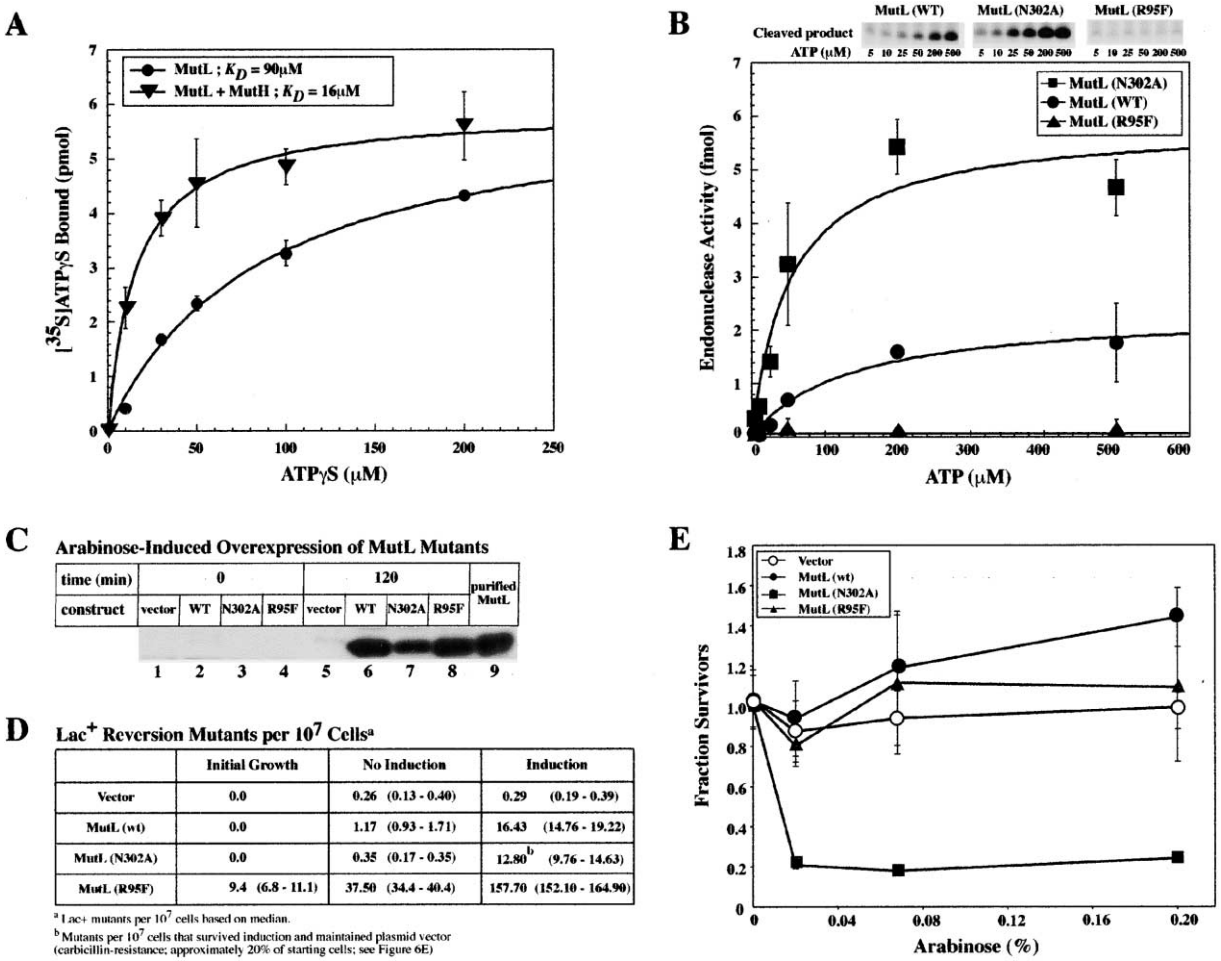

Figure 6. Activation of MutL ATP Binding by MutH and Consequent Enhancement of the MutH Endonuclease Activity

(A) The MutH protein enhanced ATPγS binding by MutL. Filter binding was used to calculate the equilibrium disassociation constants (K_D) for [^{35}S]-ATPγS binding to MutL (●) (K_D = 90 μM) and MutL plus MutH (▼) (K_D = 16 μM).

(B) Activation of MutH endonuclease by MutL mutant proteins. MutH (25 nM) endonuclease activity on a 40 bp DNA containing a single hemimethylated GATC site DNA was monitored in the presence of 500 nM wild-type and mutant MutL proteins at varying concentrations of ATP. The 20 nt ssDNA product was analyzed on denaturing urea/PAGE and visualized by PhosphorImager. The amount of product was quantitated and endonuclease activity (femtomole product) plotted as a function of ATP concentration for wild-type MutL (●), MutL(N302A) (■), and MutL(R95F) (▲) proteins. A representative product analysis is shown at the top of the graph. Standard deviation was calculated from at least three independent experiments.

(C) Western analysis of wild-type and mutant MutL following arabinose induction. Wild-type and mutant MutL proteins were placed under the control of the arabinose-inducible promoter (pBAD) and introduced into an *E. coli mutL* strain. Protein overexpression was induced by growth in 0.02% arabinose for 2 hr. Clarified protein extracts were separated by SDS/PAGE and probed with MutL antibody. Uninduced controls are shown (time 0) and purified MutL as a marker.

(D) Overexpression of wild-type and mutant MutL results in a dominant mutator phenotype. Overexpression was performed as in C in wild-type *E. coli* containing a –1 frameshift Lac$^+$ reversion marker. Mutants per 10^7 cells (median) were determined by counting the number of Lac$^+$ GC→AT revertants in cells from six independent cultures. The median values (and range) obtained for each of the proteins pre- and postinduction is shown.

(E) Survival of bacterial cells expressing wild-type and ATP binding/hydrolysis MutL mutants. The growth characteristics of cells overexpressing different MutL mutants were determined as a function of arabinose concentration. The number of cells surviving after induction was measured as a fraction of the initial number of cells inoculated in medium containing arabinose.

tion-suppression activities of MutL and that inappropriate activation of MutL is detrimental. A dominant mutator phenotype suggests at least two nonexclusive possibilities: (1) overexpression of MutL sequesters other MMR components, preventing them from functioning in MMR, or (2) overexpression of MutL induces rapid turnover of MutS sliding clamps, effectively disengaging the MMR signal. We currently favor the latter hypothesis because of the extraordinary dominant mutator phenotype displayed by the MutL(R95F) mutation which lacks ATP-dependent MutH activation activity but retains substantial MutS clamp turnover activity.

Discussion

Prevailing models for MMR appear founded on a wide variety of nonphysiological conditions that have significantly affected biochemical interpretation(s). Here we

have determined physiological salt conditions that maximize mismatch discrimination by the MutS ATPase as well as detail the circumstances under which the MutL ATPase forms a quantitative and functional complex with MutS. These data place significant restrictions on MMR models.

Considering Mechanisms for Mismatch Repair

Within a narrow window of salt concentration (100–160 mM) that is physiologically relevant, MutS displays significant mismatch-dependent ATPase activity that is regulated by mismatch-provoked ADP→ATP exchange. The DNA binding, ATPase, and ADP→ATP exchange activities in the presence of duplex DNA, widely used as a basis for other MMR models, appears largely to result from MutS interaction with free DNA ends, a condition that is rare in vivo. The background ATPase in the absence of DNA may reflect the intrinsic inefficiency of the system, the absence of a regulatory factor, or perhaps a mechanism to ensure MutS remains largely ADP-bound: the form with maximum mismatch discrimination.

The Hydrolysis-Dependent Translocation Model requires directional control of the MutS and/or MutL ATPase along the DNA. While it is clear that mismatch-provoked ATP binding induces the formation of MutS sliding clamps (Blackwell et al., 2001a; see Results), once these sliding clamps have transited off the mismatch and onto the adjacent duplex DNA, there are no known molecular controls capable of regulating/provoking ATP hydrolysis and/or ADP→ATP exchange. Such controls are necessary to complete the proposed two-site ATPase cycle that biases DNA translocation events away from the mismatch (Blackwell et al., 1998b). Similarly, the Static Transactivation Model appears inconsistent with a number of biochemical observations. For example, the formation of a long-lived heterotrimeric MutS-MutL-MutH complex would appear unlikely since MutL actually promotes the release of ATP-bound MutS sliding clamps from DNA (Figure 3). Perhaps a more compelling dilemma surrounds the assembly and stability of any macromolecular machine. Even models incorporating protein complexes with conformationally biased interactions should account for catastrophic dissociation during the biological event. One solution that is not apparent in either of the above models is molecular redundancy.

A Complete Molecular Switch Model for Mismatch Repair

Our results refine the original Molecular Switch Model for MMR to incorporate the dynamic and redundant properties of both MutS and MutL (Figure 7). We propose that MutS functions as a mismatch sensor (Figure 7A). Recognition of mismatched nucleotides by MutS provokes ADP→ATP exchange that defines this protein as a molecular switch (Fishel, 1998; Vale, 1996). ATP binding by MutS results in the formation of a stable hydrolysis-independent sliding clamp that is capable of diffusion for at least 1 kb along the DNA adjacent to the mismatch (Figure 7A; Supplemental Figure S2B). Following the dissociation/diffusion of one ATP-bound MutS sliding clamp from the mismatch, the site is exposed to iterative loading of multiple MutS sliding clamps (Figure 7B; Supplemental Figure S2A). Continuous loading of multiple MutS sliding clamps advances the location of the rearward diffusion reflecting-barrier for any single sliding clamp. Thus, the linear rate of sliding clamp movement away from the mismatch is likely to be substantially faster than predicted by a random walk (Mulrooney et al., 1996).

In addition to DNA ends, it is possible that normal fluctuations in duplex DNA may transiently mimic a mismatch-like structure and permit binding, ADP→ATP exchange, and clamp-formation by MutS. However, such short-lived DNA structures are unlikely to load multiple MutS sliding clamps. To minimize the biological consequences of such transient structures, we propose that a threshold number of localized ATP-bound MutS sliding clamps are required to initiate MMR. In support of this hypothesis, studies with GFP-tagged MutS and MutL

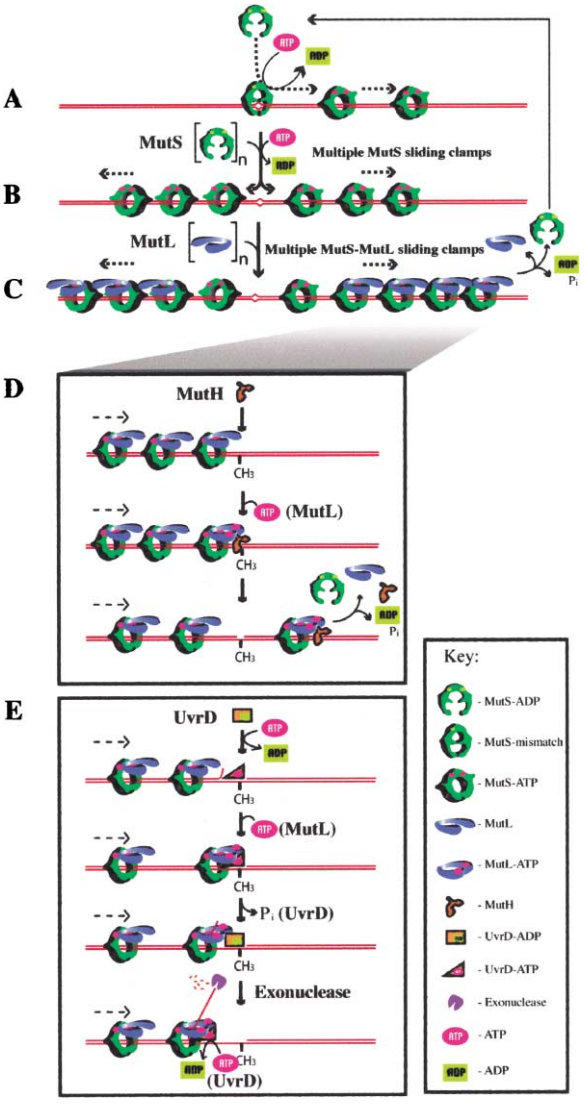

Figure 7. The Molecular Switch Model for Bacterial Mismatch Repair

See Discussion for explanation.

have visualized MMR proteins moving away from growing replication forks (Smith et al., 2001). The strong fluorescence signals seem to imply that tens to hundreds of MutS and/or MutL molecules localize to a MMR event. Multiple mismatch-localized sliding clamps solve two crucial requirements for an MMR model: mismatch recognition and DNA tracking capable of orienting the mismatch region with a downstream GATC site.

The role of MutL has been enigmatic. We show that the MutL protein only interacts with ATP-bound MutS sliding clamps (Figure 7C; Figures 3–5). We also demonstrate that the MutS-MutL complex is capable of hydrolysis-independent diffusion along DNA (Supplemental Figure S2). No qualitative difference between the diffusion properties of MutS sliding clamps and the MutS-MutL sliding clamps was observed.

Once the MutS-MutL complex is formed, MutL appears to perform two functions. First, MutL enhances the unloading of MutS sliding clamps (Figures 3D and 7C). This unexpected and unique function likely serves as an abortive reaction that removes unused sliding clamps in the absence of other key MMR components. The MutS clamp-unloading function occurs independent of ATP binding or hydrolysis by MutL (Figure 5). A second function for MutL physically connects the MutS sliding clamps to the MutH endonuclease (Figure 7D; Figure 6). The interaction with MutH protein enhances ATP binding by MutL that in turn appears to significantly enhance the endonuclease activity of MutH (Figure 6). These results define MutL as a protein-activated molecular switch.

While the exact mechanism of MutL activation of MutH endonuclease is unknown, it is likely that ATP binding by MutL results in a long-lived MutS-MutL-MutH endonuclease-competent intermediate (Figure 7D; Hall et al., 1998; Spampinato and Modrich, 2000). Interestingly, a constitutively activated mutant, MutL(N302A), induces significant cellular lethality (Figure 6D). There are at least two possible mechanisms that might contribute to lethality: (1) MutL(N302A) inappropriately activates the MutH endonuclease activity, leading to ssDNA scissions and genetic catastrophe, or (2) MutL(N302A) inappropriately interacts with some other replication and/or repair machinery, thereby decreasing cell viability.

Application of the Molecular Switch Model to the Excision of the Nascent DNA Strand

Our data do not directly address the steps following MutH endonuclease incision at a hemimethylated GATC site. However, a testable mechanism for the completion of MMR that incorporates the properties of UvrD helicase may be easily visualized (Figure 7E). The UvrD helicase initiates unwinding from a single-strand scission (Matson, 1986) and helicase processivity is significantly enhanced by the addition of MutS plus MutL (Yamaguchi et al., 1998). We consider the possibility that the UvrD helicase or a ssDNA intermediate generated during unwinding provokes ATP binding by MutL similar to that demonstrated by MutH (Figure 7E). A MutS-MutL sliding clamp linked to UvrD is appealing because of its similarity to β-clamp processivity factor and its association with the Pol III holoenzyme (O'Donnell et al., 1992). However, it would appear equally likely that MutL forms a second ATP-dependent sliding clamp that surrounds a displaced single-strand, thus stabilizing a UvrD helicase intermediate and ultimately introducing processivity.

Fundamental Redundancy

Multiple dynamic MutS-MutL sliding clamps introduce significant redundancy into the Molecular Switch Model. At any stage of the MMR process, the protein components may encounter catastrophic and/or induced dissociation. However, multiple MutS-MutL sliding clamp complexes remain associated with the residual intermediate(s) and ensure that the MMR reaction may be rapidly restarted from the last end-point. This process would appear completely iterative until the excision tract disrupts the mismatch that is responsible for the initial loading of MutS sliding clamps. The Molecular Switch Model then satisfies the final and perhaps most significant requirement of MMR: the excision tracts are directional and cover only the DNA region between GATC incision to just past the mismatch. This model appears easily adaptable to the eukaryotic MSH and MLH homologs and ultimately eukaryotic MMR.

Experimental Procedures

DNA Substrates

Oligonucleotides were synthesized by Midland Certified Reagent Company (Midland, Texas). DNA substrates for ATPase analysis (41 bp) were prepared by using the following strands (5′→3′): T-strand, CCGCTGAATTGCACCGAG CTTGATCCTCGATGATCCTA AGC; C-strand, CCGCTGAATTGCACCGAGCT**C**GATCCTCGATGAT CCTAAGC; G-strand, GCTTAGGATCATCGAGGATC**G**AGCTCGGTG CAATTCAGCGG. The site of the mismatch (G/T) or match (G/C) is indicated in bold. The G-strand was annealed to the T-strand (G/T substrate) or the C-strand (G/C substrate) in 10 mM Tris (pH 8.0), 1 mM EDTA, 500 mM NaCl. The annealed product was purified from the single strands by using BND cellulose as previously described (Gradia et al., 1997).

For ADP→ATP exchange studies, the above 41-mer strands were synthesized with a biotin linked to the 3′-end. The annealed products were purified using a HPLC on a Waters SepPak column. Double-end blocked substrates were prepared by addition of 20-fold excess streptavidin. Analysis of the blocked substrate using a 5% native PAGE indicated that more than 90% DNA was blocked on both ends. The 82 bp substrates were prepared by using the following strands: T-strand, AACTATAGGGCGAATTGGGTACCGCTGAATTG CACCGAGCTTGATCCTCGATGATCCTAAGCTAAGCTTCAGCTCC AGCTTT; C-strand, AACTATAGGGCGAATTGGGTACCGCTGAATT GCACCGAGCT**C**GATCCTCGATGATCCTAAGCTAAGCTTCAGCTC CAGCTTT; G-strand, AAAGCTGGAGCTGAAGCTTAGCTTAGGATC ATCGAGGATC**G**AGCTCGGTGCAATTCAGCGGTACCCAATTCGCC CTATAGTT. The G/T mismatch and the G/C duplex DNA were prepared by annealing the G-strand with the T-strand and the C-strand, respectively. Annealed products were purified by BND-cellulose.

For gel-shift experiments the above 82-mer strands were synthesized with a biotin group linked to the 81st nucleotide (biotinylated deoxythymidine). The annealed product was purified on a HPLC using a SepPak column. DNA was labeled by T4 polynucleotide kinase and the ends were blocked by the addition of 20-fold excess streptavidin. The double-end blocked substrate was purified by gel-extraction using native PAGE as described (Gradia et al., 1999).

For TIR IAsys studies the above 82-mer strands were synthesized with the following modifications: the G-strand contained a fluorescein group attached to the 5′-end, and the C-strand and T-strand contained a biotin group attached to the 5′-end. The T- or the C-strand was annealed with 4-fold molar excess of the G-strand. The DNA was stored at 4°C and bound to the cuvette surface as described below.

Circular DNA substrates containing a single G/T mismatch were prepared as described (Gradia et al., 1999).

DNA substrate for MutH endonuclease assay was prepared by annealing the following strands: CH_3 strand, CACTACGTGAACCAT CACTG[^{m}**A**]TCAGCGTAACGAAGAGCCC (where [^{m}**A**] refers to N-6 methyl adenine); complimentary GATC strand, GGGCTCTTCGTT ACGCTGATCAGTGATGGTTCACGTAGTG. The annealed product was purified on a Waters SepPak column by HPLC.

Protein Purification

Wild-type MutS and MutL proteins were purified as described (Galio et al., 1999; Grilley et al., 1989; Haber and Walker, 1991). His-tagged MutL mutants were purified on a Ni^{2+} affinity column (Feng and Winkler, 1995; Gradia et al., 1997), followed by chromatography on MonoQ (Feng and Winkler, 1995). His-tagged MutH was purified on Ni^{2+} affinity chromatography followed by gel filtration on S-200 and concentration on Mono Q. Proteins were dialyzed extensively against 25 mM HEPES-NaOH (pH 7.5), 100 mM NaCl, 20% glycerol, 1 mM DTT, 1 mM EDTA, snap-frozen in liquid N_2, and stored at –70°C. Western analysis was performed as previously described (Aronshtam and Marinus, 1996).

ATPase Assays

The ATPase activity of MutS was measured in a reaction buffer (20 μl) containing 25 mM HEPES-NaOH (pH 7.5), 1 mM DTT, 10 mM $MgCl_2$, 15% glycerol, 50 μg/ml BSA, 140 mM NaCl (except where indicated), 0.5 mM ATP, and 16.5 nM [$\gamma-^{32}$P] ATP. Reactions were performed at 37°C for 30 min and stopped by the addition of 400 μl of 10% activated charcoal (Norit) containing 1 mM EDTA. Norit was removed by centrifugation and 100 μl aliquots of the supernatant were counted by liquid scintillation to measure the released phosphate. Standard of deviation was calculated from at least three independent experiments.

ADP→ATP Exchange

ADP→ATP exchange was performed as previously described (Gradia et al., 1997). The MutS protein (100 nM) was preincubated in Buffer A (25 mM HEPES-NaOH [pH 7.5], 1 mM DTT, 15% glycerol, 10 mM $MgCl_2$, 100 μg/ml acetylated BSA, 100 mM NaCl) containing 3.0 μM [^{3}H]-ADP at 23°C for 10 min. Reactions were then placed on ice. We noted that bound [^{3}H]-ADP was stable (±1%) on ice for up to 2 hr. To measure ADP→ATP exchange, an equal volume of Buffer A containing 50 μM ATP was added and the reaction incubated at 23°C for indicated times. Little or no release of ADP was observed in the absence of exogenous ATP. The reaction was stopped by diluting with 3 ml ice-cold stop buffer (25 mM HEPES-NaOH [pH 7.5], 10 mM $MgCl_2$, 100 mM NaCl) and immediately filtering over a prerinsed Millipore HAWP nitrocellulose membrane. The filters were washed with 3 ml of ice-cold stop buffer, air dried, and equilibrated overnight in 4 ml scintillation fluid (Scintiverse, Fisher Scientific) before counting. Standard of deviation was calculated from at least three independent experiments.

ATPγS Binding

Binding of ATPγS was measured in Buffer A containing 12% glycerol. MMR proteins (1.0 μM) were incubated at 37°C for 30 min in Buffer A containing ATPγS concentrations as indicated, supplemented with 0.3 μM [^{35}S]-ATPγS. Reactions were placed on ice for 30 min and filtered as described for ADP→ATP exchange studies. Filters were dried and counted as described above. Standard deviation was calculated from at least three independent experiments.

Gel Shift Analysis

DNA substrate binding (20 μl) was performed in Buffer A containing 50 μg/ml BSA, 100 ng polydI-dC, 25 μM ADP, and 10 fmol [^{32}P]-labeled DNA. Reactions were initiated by the addition of MutS (100 nM) and incubation at 37°C for 5 min. This was followed by sequential addition and incubation of reagents in the following order (where indicated): ATP or ATPγS (1 mM, 10 min), MutL (100 nM, 10 min). Competitor DNA or ScaI endonuclease was then added as required and the incubation continued for an additional 10 min. Reactions with 82 bp oligonucleotide substrate were separated at 4°C on 5% native PAGE in Tris-borate buffer at 25 mA for 2 hr (Maniatis et al., 1982). Reactions with circular DNA were analyzed by electrophoresis on 1% agarose gel in Tris-Acetate buffer at 80 V for 90 min (Maniatis et al., 1982). Gels were dried and exposed to a phosphorimager (Molecular Dynamics). The results are representative of at least three independent experiments.

Total Internal Reflectance

Real-time total internal reflectance (TIR) analysis was performed using the IAsys (Affinity Sensors). A biotin-coated cuvette measurement surface was used for the analysis in Buffer B (25 mM HEPES-NaOH [pH 7.5], 10 mM $MgCl_2$, 110 mM NaCl, 1mM DTT, 2% glycerol, 150 μg/ml BSA). Streptavidin was bound to the cuvette surface and the increase in response units followed until equilibrium was established (3–5 min). Excess streptavidin was removed with repeated washing with phosphate buffered saline (PBS [Maniatis et al., 1982]). The 82 bp DNA substrate containing 5′ fluorescein on the G-strand and 5′ biotin on the complimentary T-strand (G/T mismatch DNA) or C-strand (G/C duplex DNA) was added to streptavidin-coated cuvette, equilibrium of response units established, and unbound DNA removed by repeated washing with PBS. In reactions using double-end blocked DNA, the 5′-fluorescein end was blocked using anti-fluorescein Fab fragment (0.4 μg; Molecular Probes, Eugene, OR). The anti-fluorescein Fab fragment (0.4 μg) was retained in all the subsequent buffers. The cuvette was then equilibrated with Buffer B prior to binding analysis. Binding was initiated by the addition of MutS (200 nM) in the Buffer B containing 25 μM ADP (30 μl), and the change in response units followed until equilibrium was established. We found that the addition of 25 μM ADP did not alter the kinetics or total binding of MutS to the G/T mismatch DNA. Unbound protein was removed in the "replace" mode by replacing the binding buffer with fresh Buffer B without protein or nucleotide (30 μl). MutS release was performed by adding ATP or ATPγS (1 mM) in Buffer B (30 μl). Unbound protein and free nucleotide were removed and replaced with fresh Buffer B (30 μl). MutL association was performed in the "retain" mode. The MutL (200 nM final) protein was added in Buffer B (30 μl) containing the appropriate nucleotide and the binding monitored for 10 min. We noted that the addition of Buffer B (30 μl) without MutL did not significantly alter the level of response units (bound material) over a 10 min period. The 82 bp G/T competitor DNA was then added (15 μl) in the same buffer and monitored for 10 min. The resultant curves were imported from the original data using FAST-PLOT software (Affinity Sensors, Cambridge, UK).

MutH Endonuclease

MutH endonuclease activity was measured in Buffer C (25 mM HEPES-NaOH [pH 7.5], 1 mM DTT, 18% glycerol, 10 mM $MgCl_2$, 135 μg/ml acetylated BSA, 100 mM NaCl, 5 nM [^{32}P]-DNA substrate). Reactions were initiated by the addition of the MutH (25 nM) and MutL (500 nM) proteins, varying ATP concentrations (as indicated), and incubating at 23°C for 1 hr. An equal volume of endonuclease stop solution (80% formamide, 10 mM EDTA) was added to stop the reaction. Reactions were heated to 95°C for 2 min and products separated on a 15% denaturing urea-PAGE (Maniatis et al., 1982). Endonuclease products were quantitated by Phosphorimager (Molecular Dynamics). The amount of endonuclease product (in femtomoles) was determined. Standard deviation was calculated from at least three independent experiments.

Media

Cells were grown in LB medium (Miller, 1992) or minimal medium consisting of M9 salts (Miller, 1992) plus 0.1% or 0.01% glycerol (Gly), solidified with 1.5% agar when appropriate. Carbenicillin (Carb) was added to rich medium at 100 μg/ml and to minimal medium at 50 μg/ml. For transcriptional induction, 0.02 to 0.2% arabinose (Ara) was added to M9 Gly medium. Lac$^+$ revertants were selected on solid M9 plus 0.1% lactose (Lac) medium.

Mutation Frequency

Strain CC108 (Cupples et al., 1990) was transformed with the vector, pBAD24 (Guzman et al., 1995), pKM157 (pBAD24-mutL$^+$, obtained from M. Marinus), pBAD24-N302A, and pBAD24-R95F. The resulting strains were grown to saturation in M9 0.1% Gly plus Carb. Each culture was diluted 10^5-fold into M9 0.01% Gly plus Carb, and 200 μl aliquots (containing $\sim 4 \times 10^3$ cells) dispensed into each of 24

microtiter wells. These cultures were grown for 72 hr at 37°C, then 50 μl from each microtiter well (containing approximately 7×10^6 cells) was added to 50 μl of M9 0.1% Gly plus 50 μg/ml Carb with and without 0.02% Ara. The remaining 100 μl of each primary culture was used to measure cell growth and mutation as described below for the secondary cultures. The secondary cultures were grown for an additional 72 hr at 37°C. Five microliter aliquots were removed from six wells into M9 salts and appropriate dilutions plated on LB and LB plus Carb to determine the cell numbers. The entire contents of the microwells were mixed with 2×10^9 cells of strain FC755 (a nonreverting Lac⁻ scavenger strain) and plated in minimal top agar on solid M9 plus Lac medium. Lac⁺ colonies were counted after the plates were incubated for 48 hr at 37°C. During the second growth period, without Ara, the cell numbers of all the strains increased 10-fold; with Ara, the cells carrying the vector increased 10-fold, cells carrying mutL⁺ or R95F increased 5-fold, and the cells carrying N302A increased 5-fold if titered on LB, but did not increase at all if titered on LB plus Carb (see Figure 6C). The mutation rates of the strains did not change during the second growth under noninducing conditions. The results in Figure 6C are the median number of Lac⁺ colonies divided by the number of cells as determined on LB plus Carb.

Survival under Inducing Conditions

The four strains were grown to saturation in M9 0.1% Gly plus Carb and diluted 10^5-fold into the same medium; 100 μl aliquots (containing approximately 2×10^3 cells) were dispensed into 12 microtiter wells. After incubating for 72 hr at 37°C, 4 wells were combined, to give 3 samples for each strain, and plated at various dilutions on solid M9 0.1% Gly plus Carb plus 0, 0.02, 0.068, and 0.2% Ara. Surviving colonies were counted after the plates were incubated for 48 hr at 37°C. The ratios of the number of survivors at each arabinose concentration to the number of cells at 0% Ara are given in Figure 6E. Because both numbers have associated errors, these ratios and the standard errors for the ratios were calculated using the formula found in Rice (1995).

Acknowledgments

The authors wish to thank Ron Fox and Richard Kolodner for helpful comments, Kristine Yoder for multiple discussions and editorial assistance, Anthony Mazurek for help with kinetic analysis, Martin Marinus for pKM109 and MutL antibody, Charles Marcaillou for expert technical assistance, and two anonymous reviewers for insightful and rigorous critiques. P.B. is on a leave of absence from the Centre National de Recherche Scientifique. This work was supported by National Institutes of Health grants CA67007 (R.F.) and GM54084/GM065175 (R.L.F.).

Received: November 7, 2002
Revised: April 10, 2003
Accepted: May 1, 2003
Published online: June 2, 2003

References

Alani, E., Sokolsky, T., Studamire, B., Miret, J.J., and Lahue, R.S. (1997). Genetic and biochemical analysis of Msh2p-Msh6p: role of ATP hydrolysis and Msh2p-Msh6p subunit interactions in mismatch base pair recognition. Mol. Cell. Biol. *17*, 2436–2447.

Allen, D.J., Makhov, A., Grilley, M., Taylor, J., Thresher, R., Modrich, P., and Griffith, J.D. (1997). MutS mediates heteroduplex loop formation by a translocation mechanism. EMBO J. *16*, 4467–4476.

Aronshtam, A., and Marinus, M.G. (1996). Dominant negative mutator mutations in the mutL gene of *Escherichia coli*. Nucleic Acids Res. *24*, 2498–2504.

Ban, C., Junop, M., and Yang, W. (1999). Transformation of MutL by ATP binding and hydrolysis: a switch in DNA mismatch repair. Cell *97*, 85–97.

Ban, C., and Yang, W. (1998a). Crystal structure and ATPase activity of MutL: Implications for DNA repair and mutagenesis. Cell *95*, 541–552.

Ban, C., and Yang, W. (1998b). Structural basis for MutH activation in *E.coli* mismatch repair and relationship of MutH to restriction endonucleases. EMBO J. *17*, 1526–1534.

Berger, J.M., and Wang, J.C. (1996). Recent developments in DNA topoisomerase II structure and mechanism. Curr. Opin. Struct. Biol. *6*, 84–90.

Bergerat, A., de Massy, B., Gadelle, D., Varoutas, P.C., Nicolas, A., and Forterre, P. (1997). An atypical topoisomerase II from Archaea with implications for meiotic recombination. Nature *386*, 414–417.

Biswas, I., Obmolova, G., Takahashi, M., Herr, A., Newman, M.A., Yang, W., and Hsieh, P. (2001). Disruption of the helix-u-turn-helix motif of MutS protein: loss of subunit dimerization, mismatch binding and ATP hydrolysis. J. Mol. Biol. *305*, 805–816.

Blackwell, L.J., Bjornson, K.P., and Modrich, P. (1998a). DNA-dependent activation of the hMutSα ATPase. J. Biol. Chem. *273*, 32049–32054.

Blackwell, L.J., Martik, D., Bjornson, K.P., Bjornson, E.S., and Modrich, P. (1998b). Nucleotide-promoted release of hMutSα from heteroduplex DNA is consistent with an ATP-dependent translocation mechanism. J. Biol. Chem. *273*, 32055–32062.

Blackwell, L.J., Bjornson, K.P., Allen, D.J., and Modrich, P. (2001a). Distinct MutS DNA-binding modes that are differentially modulated by ATP binding and hydrolysis. J. Biol. Chem. *276*, 34339–34347.

Blackwell, L.J., Wang, S., and Modrich, P. (2001b). DNA chain length dependence of formation and dynamics of hMutSα·hMutLα heteroduplex complexes. J. Biol. Chem. *276*, 33233–33240.

Cooper, D.L., Lahue, R.S., and Modrich, P. (1993). Methyl-directed mismatch repair is bidirectional. J. Biol. Chem. *268*, 11823–11829.

Cupples, C.G., Cabrera, M., Cruz, C., and Miller, J.H. (1990). A set of *lacZ* mutations in *Escherichia coli* that allow rapid detection of specific frameshift mutations. Genetics *125*, 275–280.

Drotschmann, K., Yang, W., and Kunkel, T.A. (2002). Evidence for sequential action of two ATPase active sites in yeast Msh2–Msh6. DNA Repair *1*, 743–753.

Feng, G., and Winkler, M.E. (1995). Single-step purifications of His6-MutH, His6-MutL and His6-MutS repair proteins of *Escherichia coli* K-12. Biotechniques *19*, 956–965.

Feng, G., Tsui, H.C., and Winkler, M.E. (1996). Depletion of the cellular amounts of the MutS and MutH methyl-directed mismatch repair proteins in stationary-phase *Escherichia coli* K-12 cells. J. Bacteriol. *178*, 2388–2396.

Fishel, R. (1998). Mismatch repair, molecular switches, and signal transduction. Genes Dev. *12*, 2096–2101.

Fishel, R., Acharya, S., Berardini, M., Bocker, T., Charbonneau, N., Cranston, A., Gradia, S., Guerrette, S., Heinen, C.D., Mazurek, A., et al. (2000). Signaling mismatch repair: the mechanics of an adenosine-nucleotide molecular switch. Cold Spring Harb. Symp. Quant. Biol. *65*, 217–224.

Galio, L., Bouquet, C., and Brooks, P. (1999). ATP hydrolysis-dependent formation of a dynamic ternary nucleoprotein complex with MutS and MutL. Nucleic Acids Res. *27*, 2325–2331.

Gradia, S., Acharya, S., and Fishel, R. (1997). The human mismatch recognition complex hMSH2-hMSH6 functions as a novel molecular switch. Cell *91*, 995–1005.

Gradia, S., Subramanian, D., Wilson, T., Acharya, S., Makhov, A., Griffith, J., and Fishel, R. (1999). hMSH2-hMSH6 forms a hydrolysis-independent sliding clamp on mismatched DNA. Mol. Cell *3*, 255–261.

Gradia, S., Acharya, S., and Fishel, R. (2000). The role of mismatched nucleotides in activating the hMSH2-hMSH6 molecular switch. J. Biol. Chem. *275*, 3922–3930.

Grilley, M., Griffith, J., and Modrich, P. (1993). Bidirectional excision in methyl-directed mismatch repair. J. Biol. Chem. *268*, 11830–11837.

Grilley, M., Welsh, K.M., Su, S.S., and Modrich, P. (1989). Isolation and characterization of the *Escherichia coli mutL* gene product. J. Biol. Chem. *264*, 1000–1004.

Gu, L., Hong, Y., McCulloch, S., Watanabe, H., and Li, G.M. (1998). ATP-dependent interaction of human mismatch repair proteins and

dual role of PCNA in mismatch repair. Nucleic Acids Res. *26*, 1173–1178.

Guerrette, S., Wilson, T., Gradia, S., and Fishel, R. (1998). Interactions of human hMSH2 with hMSH3 and hMSH2 with hMSH6: examination of mutations found in hereditary nonpolyposis colorectal cancer. Mol. Cell. Biol. *18*, 6616–6623.

Guerrette, S., Acharya, S., and Fishel, R. (1999). The interaction of the human MutL homologues in hereditary nonpolyposis colon cancer. J. Biol. Chem. *274*, 6336–6341.

Guzman, L.M., Belin, D., Carson, M.J., and Beckwith, J. (1995). Tight regulation, modulation, and high-level expression by vectors containing the arabinose PBAD promoter. J. Bacteriol. *177*, 4121–4130.

Haber, L.T., and Walker, G.C. (1991). Altering the conserved nucleotide binding motif in the *Salmonella typhimurium* MutS mismatch repair protein affects both its ATPase and mismatch binding activities. EMBO J. *10*, 2707–2715.

Habraken, Y., Sung, P., Prakash, L., and Prakash, S. (1998). ATP-dependent assembly of a ternary complex consisting of a DNA mismatch and the yeast MSH2–MSH6 and MLH1–PMS1 protein complexes. J. Biol. Chem. *273*, 9837–9841.

Hall, M.C., Jordan, J.R., and Matson, S.W. (1998). Evidence for a physical interaction between the *Escherichia coli* methyl-directed mismatch repair proteins MutL and UvrD. EMBO J. *17*, 1535–1541.

Hall, M.C., Wang, H., Erie, D.A., and Kunkel, T.A. (2001). High affinity cooperative DNA binding by the yeast Mlh1-Pms1 heterodimer. J. Mol. Biol. *312*, 637–647.

Heinen, C.D., Wilson, T., Mazurek, A., Berardini, M., Butz, C., and Fishel, R. (2002). HNPCC mutations in hMSH2 result in reduced hMSH2-hMSH6 molecular switch functions. Cancer Cell *1*, 469–478.

Hess, M.T., Gupta, R.D., and Kolodner, R.D. (2002). Dominant *Saccharomyces cerevisiae msh6* mutations cause increased mispair binding and decreased dissociation from mispairs by Msh2-Msh6 in the presence of ATP. J. Biol. Chem. *277*, 25545–25553.

Jiricny, J., Su, S.S., Wood, S.G., and Modrich, P. (1988). Mismatch-containing oligonucleotide duplexes bound by the *E. coli* MutS-encoded protein. Nucleic Acids Res. *16*, 7843–7853.

Junop, M.S., Obmolova, G., Rausch, K., Hsieh, P., and Yang, W. (2001). Composite active site of an ABC ATPase: MutS uses ATP to verify mismatch recognition and authorize DNA repair. Mol. Cell *7*, 1–12.

Kolodner, R. (1996). Biochemistry and genetics of eukaryotic mismatch repair. Genes Dev. *10*, 1433–1442.

Lahue, R.S., Au, K.G., and Modrich, P. (1989). DNA mismatch correction in a defined system. Science *245*, 160–164.

Lamers, M.H., Perrakis, A., Enzlin, J.H., Winterwerp, H.H., de Wind, N., and Sixma, T.K. (2000). The crystal structure of DNA mismatch repair protein MutS binding to a G·T mismatch. Nature *407*, 711–717.

Maniatis, T., Fritsch, E.F., and Sambrook, J. (1982). Molecular Cloning (Cold Spring Harbor, NY: Cold Spring Harbor Laboratory Press).

Matson, S.W. (1986). *Escherichia coli* helicase II (*uvrD* gene product) translocates unidirectionally in a 3′ to 5′ direction. J. Biol. Chem. *261*, 10169–10175.

Miller, J.H. (1992). Experiments in Molecular Genetics (Cold Spring Harbor, NY: Cold Spring Harbor Laboratory Press)

Modrich, P. (1989). Methyl-directed DNA mismatch correction. J. Biol. Chem. *264*, 6597–6600.

Modrich, P., and Lahue, R. (1996). Mismatch repair in replication fidelity, genetic recombination, and cancer biology. Annu. Rev. Biochem. *65*, 101–133.

Muller, A., and Fishel, R. (2002). Mismatch repair and the hereditary non-polyposis colorectal cancer syndrome (HNPCC). Cancer Invest. *20*, 102–109.

Mulrooney, S.B., Fishel, R.A., Hejna, J.A., and Warner, R.C. (1996). Preparation of figure 8 and cruciform DNAs and their use in studies of the kinetics of branch migration. J. Biol. Chem. *271*, 9648–9659.

Mushegian, A.R., Bassett, D.E., Jr., Boguski, M.S., Bork, P., and Koonin, E.V. (1997). Positionally cloned human disease genes: Patterns of evolutionary conservation and functional motifs. Proc. Natl. Acad. Sci. USA *94*, 5831–5836.

O'Donnell, M., Kuriyan, J., Kong, X.P., Stukenberg, P.T., and Onrust, R. (1992). The sliding clamp of DNA polymerase III holoenzyme encircles DNA. Mol. Biol. Cell *3*, 953–957.

Obmolova, G., Ban, C., Hsieh, P., and Yang, W. (2000). Crystal structures of mismatch repair protein MutS and its complex with a substrate DNA. Nature *407*, 703–710.

Plotz, G., Raedle, J., Brieger, A., Trojan, J., and Zeuzem, S. (2002). hMutSα forms an ATP-dependent complex with hMutLα and hMutLβ on DNA. Nucleic Acids Res. *30*, 711–718.

Prolla, T.A., Pang, Q., Alani, E., Kolodner, R.D., and Liskay, R.M. (1994). MLH1, PMS1, and MSH2 interactions during the initiation of DNA mismatch repair in yeast. Science *265*, 1091–1093.

Raschle, M., Dufner, P., Marra, G., and Jiricny, J. (2002). Mutations within the hMLH1 and hPMS2 subunits of the human MutLα mismatch repair factor affect its ATPase activity, but not its ability to interact with hMutSα. J. Biol. Chem. *277*, 21810–21820.

Record, M.T., Jr., Courtenay, E.S., Cayley, S., and Guttman, H.J. (1998). Biophysical compensation mechanisms buffering *E. coli* protein-nucleic acid interactions against changing environments. Trends Biochem. Sci. *23*, 190–194.

Rice, J. (1995). Mathematical Statistics and Data Analysis (Belmont, CA: Wadsworth Publishing Company).

Schofield, M.J., Nayak, S., Scott, T.H., Du, C., and Hsieh, P. (2001). Interaction of *Escherichia coli* MutS and MutL at a DNA mismatch. J. Biol. Chem. *276*, 28291–28299.

Schultz, S.G., and Solomon, A.K. (1961). Cation transport in *Escherichia coli*. I. Intracellular Na^+ and K^+ concentrations and net cation movemement. J. Gen. Physiol. *45*, 355–369.

Smith, B.T., Grossman, A.D., and Walker, G.C. (2001). Visualization of mismatch repair in bacterial cells. Mol. Cell *8*, 1197–1206.

Spampinato, C., and Modrich, P. (2000). The MutL ATPase is required for mismatch repair. J. Biol. Chem. *275*, 9863–9869.

Sprang, S.R. (1997). G protein mechanisms: insights from structural analysis. Annu. Rev. Biochem. *66*, 639–678.

Su, S.-S., and Modrich, P. (1986). *Escherichia coli mutS*-encoded protein binds to mismatched DNA base pairs. Proc. Natl. Acad. Sci. USA *83*, 5057–5061.

Tran, P.T., and Liskay, R.M. (2000). Functional studies on the candidate ATPase domains of *Saccharomyces cerevisiae* MutLα. Mol. Cell. Biol. *20*, 6390–6398.

Vale, R.D. (1996). Switches, latches, and amplifiers: common themes of G proteins and molecular motors. J. Cell Biol. *135*, 291–302.

Viswanathan, M., and Lovett, S.T. (1998). Single-strand DNA-specific exonucleases in *Escherichia coli* - roles in repair and mutation avoidance. Genetics *149*, 7–16.

Walker, J.E., Saraste, M., Runswick, M.J., and Gay, N.J. (1982). Distantly related sequences in the α- and β-subunits of ATP synthase, myosin, kinases and other ATP-requiring enzymes and a common nucleotide-binding fold. EMBO J. *1*, 945–951.

Welsh, K.M., Lu, A.L., Clark, S., and Modrich, P. (1987). Isolation and characterization of the *Escherichia coli mutH* gene product. J. Biol. Chem. *262*, 15624–15629.

Wilson, T., Guerrette, S., and Fishel, R. (1999). Dissociation of mismatch recognition and ATPase activity by hMSH2-hMSH3. J. Biol. Chem. *274*, 21659–21644.

Yamaguchi, M., Dao, V., and Modrich, P. (1998). MutS and MutL activate DNA helicase II in a mismatch-dependent manner. J. Biol. Chem. *273*, 9197–9201.